Facile multipoint nanoholes array-based plasmonic platform: Development, characterization, and sensor evaluation

Bento Pereira Cabral Júnior, Jean Halison de Oliveira, Paulo Henrique Maciel Buzzetti, Maiara Mitiko Taniguchi, Johny Paulo Monteiro, Luís Henrique Cardozo Amorin, Alexandre Urbano, Eduardo Radovanovic, Emerson Marcelo Girotto

Facile Multipoint Nanoholes Array-Based Plasmonic Platform: Development, Characterization, and Sensor Evaluation

Bento Pereira Cabral Júnior[a], Jean Halison de Oliveira[a], Paulo Henrique Maciel Buzzetti[a], Maiara Mitiko Taniguchi[a], Johny Paulo Monteiro[b], Luís Henrique Cardozo Amorin[c], Alexandre Urbano[c], Eduardo Radovanovic[a], Emerson Marcelo Girotto[a*]

[a] *Department of Chemistry, State University of Maringá, Maringá, PR, Brazil.*

[b] *Department of Chemistry, Federal Technological University of Paraná, Apucarana, PR, Brazil.*

[c] *Department of Physics, State University of Londrina, Londrina, PR, Brazil*

**Correspondent Author. E-mail address: emgirotto@uem.br.*

Abstract

This study demonstrates a novel nanoholes array-based plasmonic platform with potential for application in multi-detection analysis. The nanostructured transducer was obtained by nanosphere lithography (NSL), which was restricted to having a sensing multipoint. The microscopic characterization showed sensing point (Sen-P) arrays with *ca.* 380 µm and nanoholes with 234.1 ± 27.3 nm diameter. Nanoholes array transmission spectra presented a plasmonic band in *ca.* 531 nm when the refractive index (RI) was 1.3397. The plasmonic device showed a RI sensitivity of 271.92 ± 14.92 nm/RIU and could detect the bovine serum albumin (BSA) with good feasibility. These results suggest the potential suitability of our platform to develop multiple monitoring systems.

Keywords: biosensor, plasmonic holes, NSL, polymer resin, biodetection.

1. Introduction

Surface plasmon resonance (SPR)-based biosensors measure the RI changes on a metallic-dielectric interface due to biomolecular bond (analyte-bioreceptor) events. These devices have attracted great interest in label-free methods in the last decades [1]. In particular, the devices that use nanohole arrays demonstrate high sensibility, and great potential for miniaturized sensor production [2]. Another distinguishing feature is obtaining nanoholes with high control in strategic points on the metallic film. This enables the integration with microfluidic systems to get automatic and multipoint analysis, which is an important feature for the future SPR biosensor technology [3]. Moreover, the nanoholes arrays can be projected with a specific optic characteristic, controlling the hole diameter, geometry, and periodicity [4].

The cost-effectivity of nanoholes production may make their use difficult on a large scale due to the high-cost beam lithography techniques often used for nanoholes obtention, such as focused ion beam (FIB) and electron beam lithography (EBL). As an alternative, many authors have used nanospheres lithography (NSL). The accessible sphere self-assembly makes possible the development of different structures [5]. For example, the sphere volume can be adjusted by reactive ion etching (RIE) [6]. Thus, NSL has been used to prepare plasmonic biosensors based on nanoholes [7], nanowires [8], and others [9].

The NSL can thus provide a direct approach to overcoming the high cost of SPR biosensors. Thus, in this work, we prepared an unprecedented plasmonic platform based on a glass substrate covered with nanoholed gold thin film. The holes were obtained over the entire metallic surface by NSL. This technique does not enable to have nanoholes arrays in specific positions on the substrate. Thus, our main challenge was restricting the nanoholed substrate to have a particular structure of Sen-Ps on the substrate. The plasmonic platform had its sensitivity characterized, and it was tested for BSA detection.

2. Experimental section

A glass substrate covered with an entire-nanoholed gold film (Figure 1A) fabricated by NSL (support information) was used to develop a sensing multiple-point plasmonic device. Firstly, the substrate was spin-coated at 500 rpm for 40 s and ramping at 1500 rpm for 15 s (G3P-8) with a polymeric solution containing urethane dimethacrylate (UDMA, Aldrich, 100%), 2-(N, N-dimethylamino) ethyl methacrylate (DMAEMA, sigma-Aldrich, 100%), and

camphorquinone (CQ, Sigma-Aldrich, 97%) at the 85:10:5 wt% ratio (Figure 1B). The polymeric solution was degassed before its use. Then, the Sen-Ps were obtained on the specific regions of the substrate by photopolymerization. For that, a photomask containing transparent circles of 150 μm diameter (printed in polyethylene terephthalate sheets with a high-resolution printer) was positioned on the polymeric film and exposed to cure using LED curing light (Radii-cal, 440-480 nm, 1200 mW/cm^2) for 1 min (Figure 1C). The polymer on the regions unexposed to light was removed using ethanol P.A. (synth) (Figure 1D). Then, using a *sputtering* (Sputter coater SCD 050, Baltec, Canonsburg, USA), a second optically dense gold layer was deposited onto the polymeric-recovered substrate using a current of 60 mA for 240 s (Figure 1E). Finally, the polymeric coating was removed by a THF bath (Neon, 99,0 wt%) for ~2 min (Figure 1F). Morphological characterizations were performed by scanning electron microscopy (SEM, FEI Quanta 250), and the structure size was measured using Image-Pro® PLUS (version 4.5.0.29) software. The sensibility was characterized by UV-Vis spectroscopy (Ocean Optics, USB2000 with resolution of 0.1 nm), coupled to a metallographic microscope (Quimis 9738 MIT with halogen lamp of 250 W) (Figure S1). The plasmonic sensitivity to RI changes was conducted by exposing the substrate surface to glucose solutions (Sigma-Aldrich, 99,5%) with different RIs (1.3397-1.3970). The substrate biodetection capability was tested using BSA as a model biomolecule by the following procedure: 0.5 mmol/L of 11-mercaptoundecanoic acid (MUA, Sigma-Aldrich, ~95%) in ethanol covered the plasmonic substrate for 6 h. Subsequently, the rinsed sensor was added to a 1:1 aqueous solution containing N-ethyl-N-(3-diethylaminopropyl) carbodiimide (EDC, Sigma–Aldrich, ≥97%) 0.1 mol/L and N-hydroxysuccinimide (NHS, Sigma–Aldrich, ≥99%) 0.1 mol/L for 4 h. Finally, 0.5 μg/mL of BSA (Sigma–Aldrich 96%) in PBS was passed through the device for 6 h.

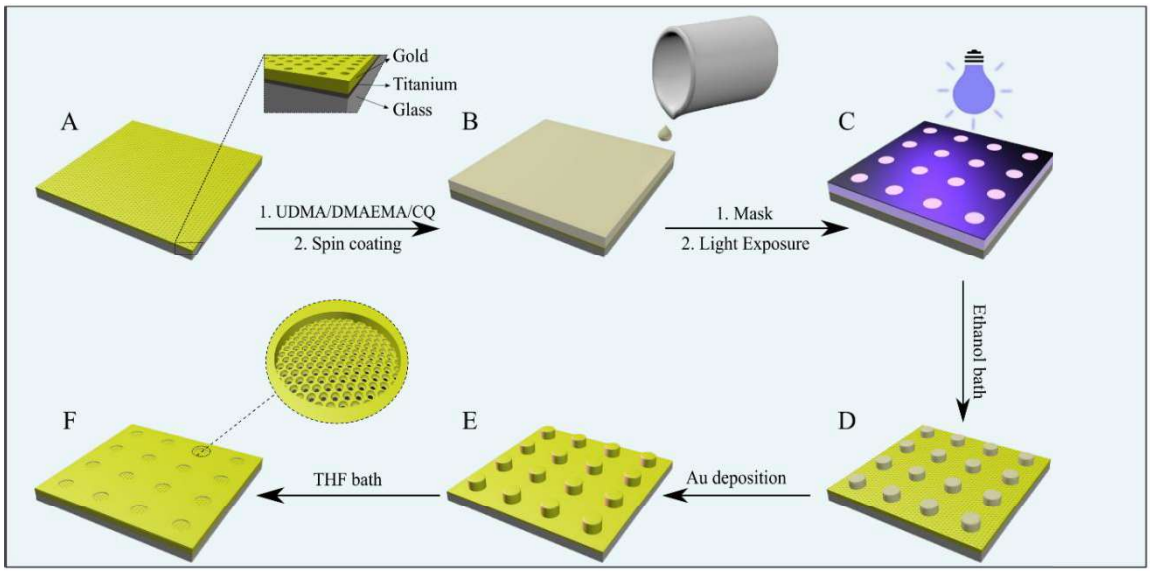

Fig. 1. Preparation process of the nanohole array-based plasmonic platform containing multiple Sen-Ps.

3. Results and discussion

Figure 2(A) shows a digital image of the demarcated substrate. The substrate had a 2.25 cm^2 total area containing around 250 circular demarcations, called "sensing points (Sen-Ps)", which are perfectly organized (bright spots in the image). The Sen-P arrays on the substrate can be customized just by changing the printed photomask design. Figure 2(B) shows an SEM image of a set of four Sen-Ps (highlighted in Fig. 1(A)) with a 380 µm diameter. The difference between the photomask transparent circular area (150 µm) and the actual area obtained for the Sen-Ps on the substrate (380 nm) can be attributed to the photopolymerization side-propagation [10]. Furthermore, light may enter beyond the edges of the transparent photomask due to a not fully collimated light beam. SEM images at different magnifications were obtained from a Sen-P and are shown in Figures 2(C)-2(D). The regions are filled with hexagonal-shaped nanoholes with an average size of 234,1 ± 27,3 nm (Inset in figure 2(D)).

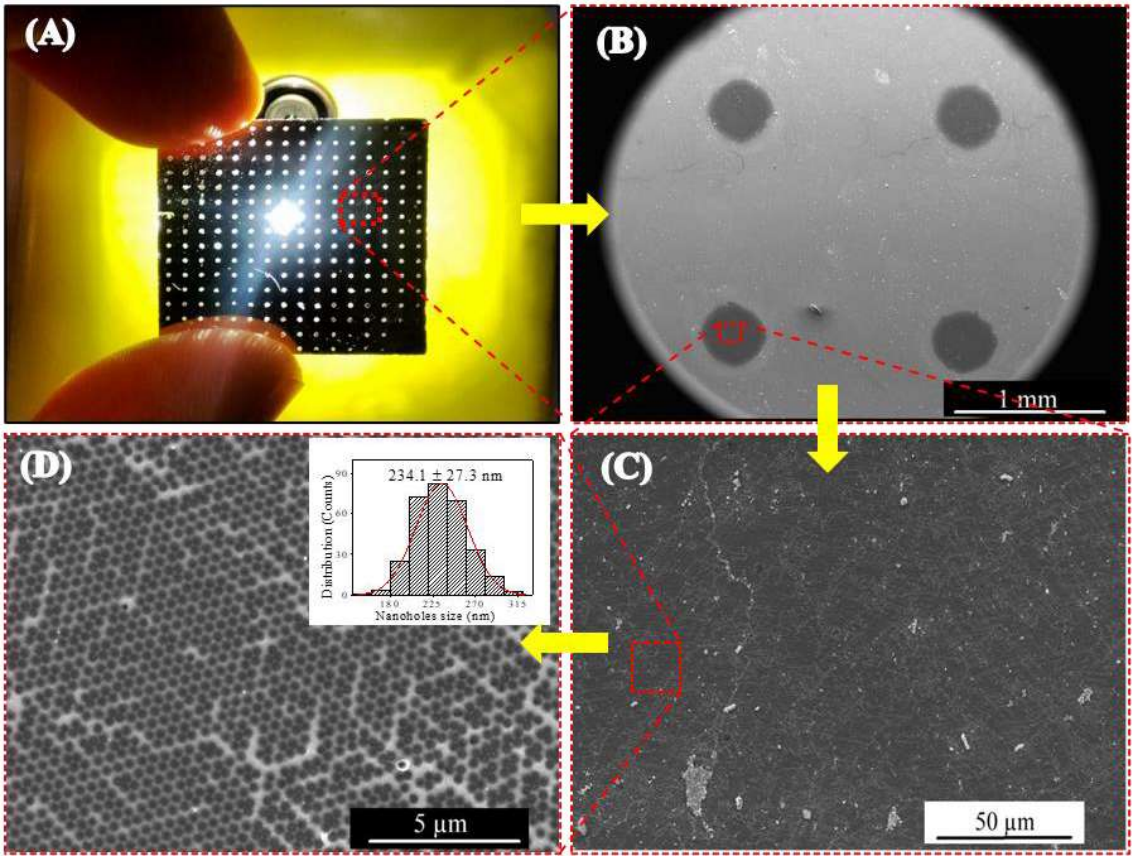

Fig. 2. (A) digital image of the demarcated substrate, (B) SEM image of the four Sen-Ps indicated in (A), and (C-D) show SEM images at different magnifications obtained within the Sen-P area. Inset in (D) shows a nanoholes size distribution obtained from the (D) image.

The evaluation of the Sen-P optical transmission revealed a plasmonic band at a 531 nm maximum wavelength when a dilute glucose solution (RI=1,3397) was on it. This behavior was the same observed for other substrate Sen-Ps. The maximum transmission wavelength was close to the one observed in our previous work [11]. As observed in Fig. 3(A)-3(B), the transmission spectra were red-shifted as the RI increased. Then, the sensitivity (S) was determined using a linear fitting of the maximum transmission wavelength as a function of RI variation. The fitting curve inclination is defined as the Sen-P sensitivity (Fig. 3(C)), which was (271.92 ± 14.92) nm/RIU. Considering that the spectrophotometer precision was 0.1 nm, the calculated resolution was 3.7 x 10^{-4} RIU. Moreover, the R^2 for the linear fitting was acceptable (0.9764), indicating that the transmission maximum wavelength shift is proportional to RI changes.

The device response to the biomolecule immobilization was also investigated using the traditional model system of MUA/NHS-BSA [12]. The MUA-NHS layers are extensively used to provide a compact layer on the gold surface [13]. The BSA aminated groups quickly adsorb

on the MUA/NHS-modified gold surface and form a 4-7 nm thick monolayer [14] (see Figure S1 in the supplementary material). Thus, this molecular system can determine the substrate's ability to evaluate the sensor surface layer-by-layer modification. This is important to define if the substrate can work as a biosensor. The Sen-P transmission spectra were acquired for each modification step. The region of the spectra maximum absorbance can be observed in Figure 3(D). The Fig. 3(D) inset shows the plasmonic band maximum wavelength for each modification. The redshift caused by the immobilization of the NHS layer over MUA was only (0.6±0.22) nm. However, a significant shift of (2.48±0.57) nm was observed when BSA molecules were immobilized on MUA-NHS layer. According to these results, and the literature support (supplementary information) the device has potential to detect surface biological interactions and also work as a plasmonic biosensor.

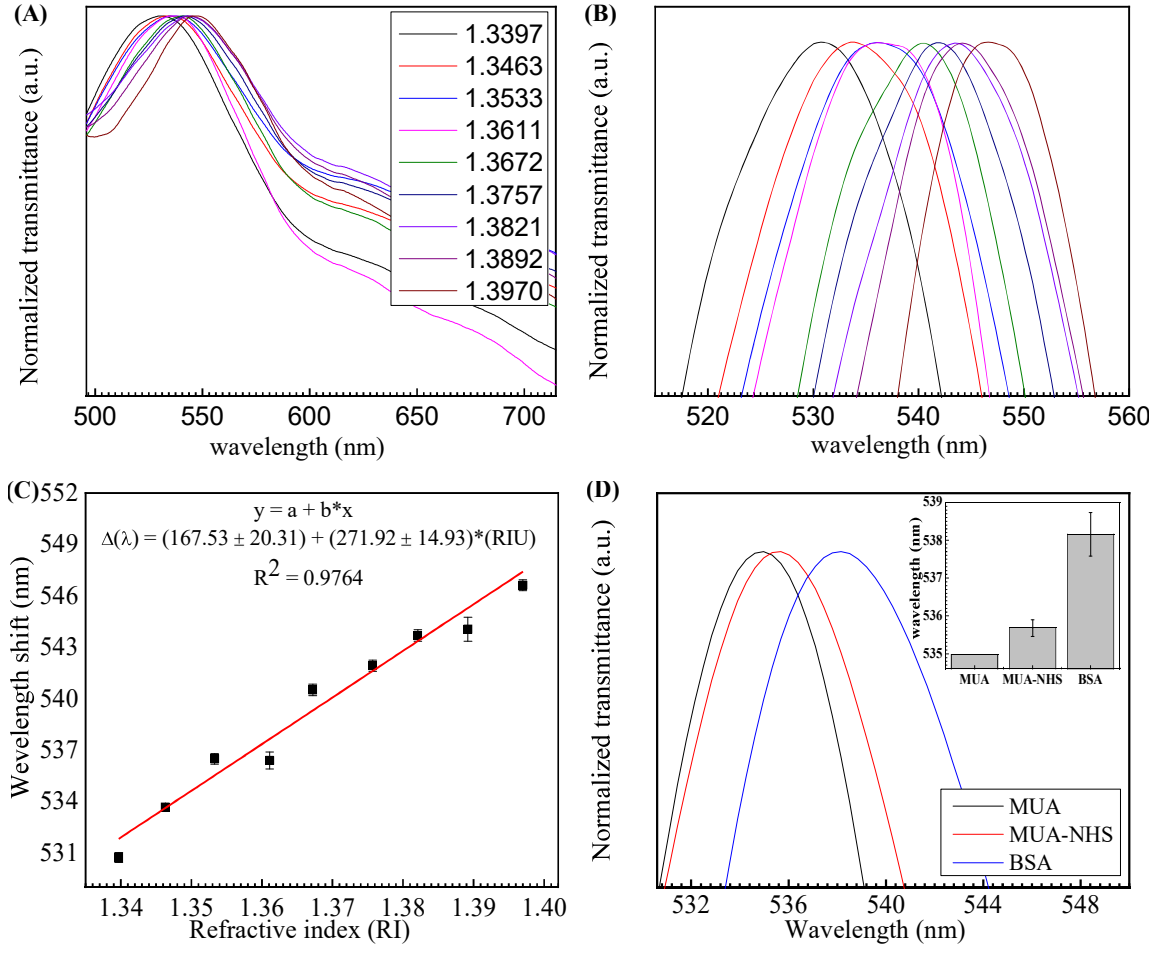

Fig. 3. (A) Transmission spectra for a Sen-P at different IRs (1.3397-1.3970). (B) Expansion of the maximum absorbance region observed in (A). (C) Maximum transmission wavelength as a function of RI variation (sensibility curve). (D) Transmission spectra for each step of the gold surface modification on the Sen-P. Inset: column chart to plasmonic band redshift.

4. Conclusion

In this work, we presented a new nanoholes-based plasmonic substrate obtained by a facile technique. The substrate was successfully prepared with several Sen-Ps with a circular area filled with hexagonal-shaped nanoholes on gold thin film. The Sen-Ps were obtained using a polymeric coating followed by remotion and then obtaining the plasmonic platform with a multiplexing potential. The Sen-P arrays can be fully customized. It was shown that the device was sensitive to RI changes and can respond to the biomolecules immobilization. The results demonstrated that combining the techniques (nanohole development by NSL and demarcation with an easy-to-remove polymeric system) enables the acquisition of plasmonic substrate with the potential for multiple detections at a label-free single device.

Acknowledgement

The authors thank the Complex of Research Support Centers (COMCAP) for equipment support, CNPq (process no. 305290/2020-7) and CAPES for fellowships.

References

[1] J. Homola, Surface Plasmon Resonance Sensors for Detection of Chemical and Biological Species, Chem. Rev. 108 (2008) 462–493. https://doi.org/10.1021/cr068107d.

[2] C. Escobedo, On-chip nanohole array-based sensing: a review, Lab Chip. 13 (2013) 2445. https://doi.org/10.1039/c3lc50107h.

[3] P.H.M. Buzzetti, M.M. Taniguchi, N.S. Mendes, R.C. Vicentino, J.H. Oliveira, B.P. Cabral Júnior, M. Souza, J.P. Monteiro, E.M. Girotto, Complete experimental and theoretical characterization of nonlinear concentration gradient generator microfluidic device for analytical purposes, Microchim. Acta. 11 (2022) 1–9. https://doi.org/10.1007/s00604-021-05110-7.

[4] A. Shalabney, I. Abdulhalim, Sensitivity-enhancement methods for surface plasmon sensors, 606 (2011) 571–606. https://doi.org/10.1002/lpor.201000009.

[5] P. Colson, C. Henrist, R. Cloots, Nanosphere Lithography: A Powerful Method for the Controlled Manufacturing of Nanomaterials, 2013 (2013) https://doi.org/10.1155/2013/948510.

158 [6] J.M. Chem, Elevated Ag nanohole arrays for high performance plasmonic sensors based
159 on extraordinary optical transmission, (2012) 8903–8910.
160 https://doi.org/10.1039/c2jm30525a.

161 [7] L. Niu, K. Cheng, Y. Wu, T. Wang, Q. Shi, D. Liu, Z. Du, Sensitivity improved
162 plasmonic gold nanoholes array biosensor by coupling quantum-dots for the detection
163 of specific biomolecular interactions, Biosens. Bioelectron. 50 (2013) 137–142.
164 https://doi.org/10.1016/j.bios.2013.06.023.

165 [8] S. Su, L. Lin, Z. Li, J. Feng, Z. Zhang, The fabrication of large-scale sub-10-nm core-
166 shell silicon nanowire arrays, Nanoscale Res. Lett. 8 (2013) 405.
167 https://doi.org/10.1186/1556-276X-8-405.

168 [9] Y. Cai, Y. Cao, P. Nordlander, P.S. Cremer, Fabrication of Split-Rings via Stretchable
169 Colloidal Lithography, ACS Photonics. 1 (2014) 127–134.
170 https://doi.org/10.1021/ph400127g.

171 [10] Z. Zhao, J. Wu, X. Mu, H. Chen, H.J. Qi, D. Fang, Origami by frontal
172 photopolymerization, Sci. Adv. 3 (2017) 1–8. https://doi.org/10.1126/sciadv.1602326.

173 [11] B.P. Cabral Júnior, J.H. Oliveira, P.H.M. Buzzetti, M.G.V. Fressatti, J.P. Monteiro,
174 L.H.C. Amorin, A. Urbano, E. Radovanovic, E.M. Girotto, Cost-effective plasmonic
175 device for label-free streptavidin detection, Mater. Lett. 227 (2018) 243–246.
176 https://doi.org/10.1016/j.matlet.2018.05.064.

177 [12] C.T.P. Silva, J.P. Monteiro, E. Radovanovic, E.M. Girotto, Unprecedented high
178 plasmonic sensitivity of substrates based on gold nanoparticles, Sensors Actuators B
179 Chem. 191 (2014) 152–157. https://doi.org/10.1016/j.snb.2013.09.109.

180 [13] J.P. Monteiro, J. Ferreira, R.G. Sabat, P. Rochon, M.J.L. Santos, E.M. Girotto, SPR
181 based biosensor using surface relief grating in transmission mode, Sensors Actuators B
182 Chem. 174 (2012) 270–273. https://doi.org/10.1016/j.snb.2012.08.026.

183 [14] H. Guner, E. Ozgur, G. Kokturk, M. Celik, E. Esen, A.E. Topal, S. Ayas, Y. Uludag, C.
184 Elbuken, A. Dana, A smartphone-based surface plasmon resonance imaging (SPRi)
185 platform for on-site biodetection, Sensors Actuators B Chem. 239 (2017) 571–577.
186 https://doi.org/10.1016/j.snb.2016.08.061.

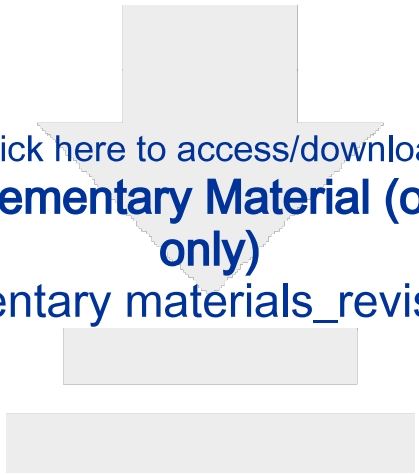

Click here to access/download

Electronic Supplementary Material (online publication only)

Supplementary materials_revised_.docx

CRediT authorship contribution statement

B. P. Cabral Júnior: Data curation, Methodology, Writing – original draft. **J. H. de Oliveira:** Formal analysis, Writing – review & editing, methodology. **J. P. Monteiro**: Conceptualization, Writing – review & editing. **P. H. M. Buzzetti**: Writing – review & editing, Investigation. **M. M. Taniguchi:** Writing – review & editing. **L. H. C. Amorin:** Methodology, Resources. **A. Urbano:** Resources. **E. Radovanovic**: Supervision, Methodology. **E. M. Girotto:** Supervision, Writing- Reviewing and Editing.

Declaration of interests

☒The authors declare that they have no known competing financial interests or personal relationships that could have appeared to influence the work reported in this paper.

☐The authors declare the following financial interests/personal relationships which may be considered as potential competing interests:

Facile Multipoint Nanoholes Array-Based Plasmonic Platform: Development, Characterization, and Sensor Evaluation

Bento Pereira Cabral Júnior[a], Jean Halison de Oliveira[a], Paulo Henrique Maciel Buzzetti[a], Maiara Mitiko Taniguchi[a], Johny Paulo Monteiro[b], Luís Henrique Cardozo Amorin[c], Alexandre Urbano[c], Eduardo Radovanovic[a], Emerson Marcelo Girotto[a*]

[a] *Department of Chemistry, State University of Maringá, Maringá, PR, Brazil.*

[b] *Department of Chemistry, Federal Technological University of Paraná, Apucarana, PR, Brazil.*

[c] *Department of Physics, State University of Londrina, Londrina, PR, Brazil*

**Correspondent Author. E-mail address: emgirotto@uem.br.*

Abstract

This study demonstrates a novel nanoholes array-based plasmonic platform with potential for application in multi-detection analysis. The nanostructured transducer was obtained by nanosphere lithography (NSL), which was restricted to having a sensing multipoint. The microscopic characterization showed sensing point (Sen-P) arrays with *ca.* 380 µm and nanoholes with 234.1 ± 27.3 nm diameter. Nanoholes array transmission spectra presented a plasmonic band in *ca.* 531 nm when the refractive index (RI) was 1.3397. The plasmonic device showed a RI sensitivity of 271.92 ± 14.92 nm/RIU and could detect the bovine serum albumin (BSA) with good feasibility. These results suggest the potential suitability of our platform to develop multiple monitoring systems.

Keywords: biosensor, plasmonic holes, NSL, polymer resin, biodetection.

1. Introduction

Surface plasmon resonance (SPR)-based biosensors measure the RI changes on a metallic-dielectric interface due to biomolecular bond (analyte-bioreceptor) events. These devices have attracted great interest in label-free methods in the last decades [1]. In particular, the devices that use nanohole arrays demonstrate high sensibility, and great potential for miniaturized sensor production [2]. Another distinguishing feature is obtaining nanoholes with high control in strategic points on the metallic film. This enables the integration with microfluidic systems to get automatic and multipoint analysis, which is an important feature for the future SPR biosensor technology [3]. Moreover, the nanoholes arrays can be projected with a specific optic characteristic, controlling the hole diameter, geometry, and periodicity [4].

The cost-effectivity of nanoholes production may make their use difficult on a large scale due to the high-cost beam lithography techniques often used for nanoholes obtention, such as focused ion beam (FIB) and electron beam lithography (EBL). As an alternative, many authors have used nanospheres lithography (NSL). The accessible sphere self-assembly makes possible the development of different structures [5]. For example, the sphere volume can be adjusted by reactive ion etching (RIE) [6]. Thus, NSL has been used to prepare plasmonic biosensors based on nanoholes [7], nanowires [8], and others [9].

The NSL can thus provide a direct approach to overcoming the high cost of SPR biosensors. Thus, in this work, we prepared an unprecedented plasmonic platform based on a glass substrate covered with nanoholed gold thin film. The holes were obtained over the entire metallic surface by NSL. This technique does not enable to have nanoholes arrays in specific positions on the substrate. Thus, our main challenge was restricting the nanoholed substrate to have a particular structure of Sen-Ps on the substrate. The plasmonic platform had its sensitivity characterized, and it was tested for BSA detection.

2. Experimental section

A glass substrate covered with an entire-nanoholed gold film (Figure 1A) fabricated by NSL (support information) was used to develop a sensing multiple-point plasmonic device. Firstly, the substrate was spin-coated at 500 rpm for 40 s and ramping at 1500 rpm for 15 s (G3P-8) with a polymeric solution containing urethane dimethacrylate (UDMA, Aldrich, 100%), 2-(N, N-dimethylamino) ethyl methacrylate (DMAEMA, sigma-Aldrich, 100%), and

camphorquinone (CQ, Sigma-Aldrich, 97%) at the 85:10:5 wt% ratio (Figure 1B). The polymeric solution was degassed before its use. Then, the Sen-Ps were obtained on the specific regions of the substrate by photopolymerization. For that, a photomask containing transparent circles of 150 μm diameter (printed in polyethylene terephthalate sheets with a high-resolution printer) was positioned on the polymeric film and exposed to cure using LED curing light (Radii-cal, 440-480 nm, 1200 mW/cm^2) for 1 min (Figure 1C). The polymer on the regions unexposed to light was removed using ethanol P.A. (synth) (Figure 1D). Then, using a *sputtering* (Sputter coater SCD 050, Baltec, Canonsburg, USA), a second optically dense gold layer was deposited onto the polymeric-recovered substrate using a current of 60 mA for 240 s (Figure 1E). Finally, the polymeric coating was removed by a THF bath (Neon, 99,0 wt%) for ~2 min (Figure 1F). Morphological characterizations were performed by scanning electron microscopy (SEM, FEI Quanta 250), and the structure size was measured using Image-Pro® PLUS (version 4.5.0.29) software. The sensibility was characterized by UV-Vis spectroscopy (Ocean Optics, USB2000 with resolution of 0.1 nm), coupled to a metallographic microscope (Quimis 9738 MIT with halogen lamp of 250 W) (Figure S1). The plasmonic sensitivity to RI changes was conducted by exposing the substrate surface to glucose solutions (Sigma-Aldrich, 99,5%) with different RIs (1.3397-1.3970). The substrate biodetection capability was tested using BSA as a model biomolecule by the following procedure: 0.5 mmol/L of 11-mercaptoundecanoic acid (MUA, Sigma-Aldrich, ~95%) in ethanol covered the plasmonic substrate for 6 h. Subsequently, the rinsed sensor was added to a 1:1 aqueous solution containing N-ethyl-N-(3-diethylaminopropyl) carbodiimide (EDC, Sigma–Aldrich, ≥97%) 0.1 mol/L and N-hydroxysuccinimide (NHS, Sigma–Aldrich, ≥99%) 0.1 mol/L for 4 h. Finally, 0.5 μg/mL of BSA (Sigma–Aldrich 96%) in PBS was passed through the device for 6 h.

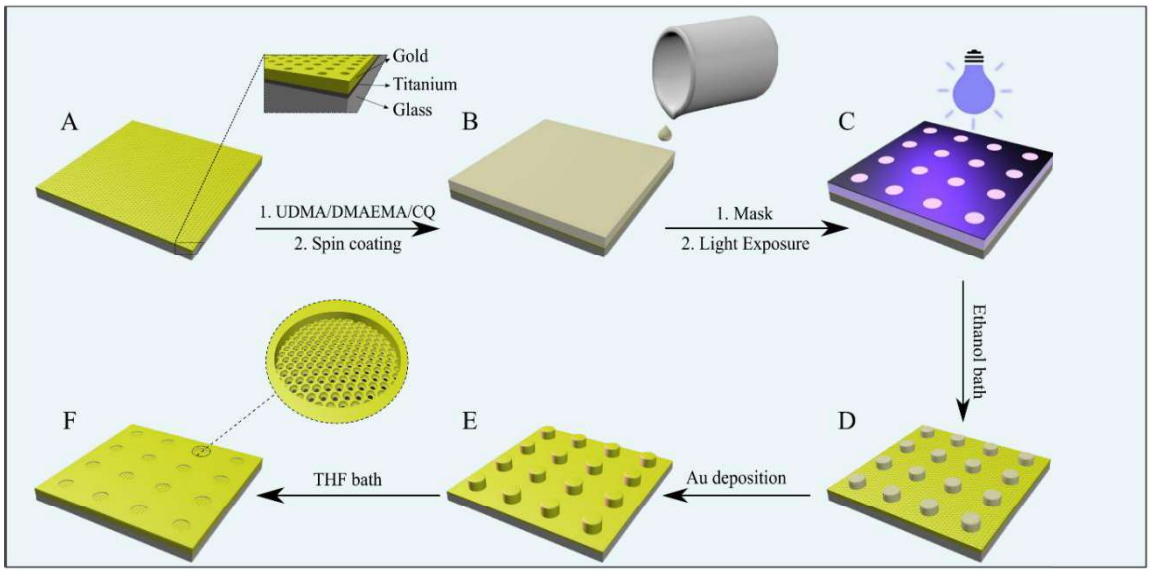

Fig. 1. Preparation process of the nanohole array-based plasmonic platform containing multiple Sen-Ps.

3. Results and discussion

Figure 2(A) shows a digital image of the demarcated substrate. The substrate had a 2.25 cm^2 total area containing around 250 circular demarcations, called "sensing points (Sen-Ps)", which are perfectly organized (bright spots in the image). The Sen-P arrays on the substrate can be customized just by changing the printed photomask design. Figure 2(B) shows an SEM image of a set of four Sen-Ps (highlighted in Fig. 1(A)) with a 380 µm diameter. The difference between the photomask transparent circular area (150 µm) and the actual area obtained for the Sen-Ps on the substrate (380 nm) can be attributed to the photopolymerization side-propagation [10]. Furthermore, light may enter beyond the edges of the transparent photomask due to a not fully collimated light beam. SEM images at different magnifications were obtained from a Sen-P and are shown in Figures 2(C)-2(D). The regions are filled with hexagonal-shaped nanoholes with an average size of 234,1 ± 27,3 nm (Inset in figure 2(D)).

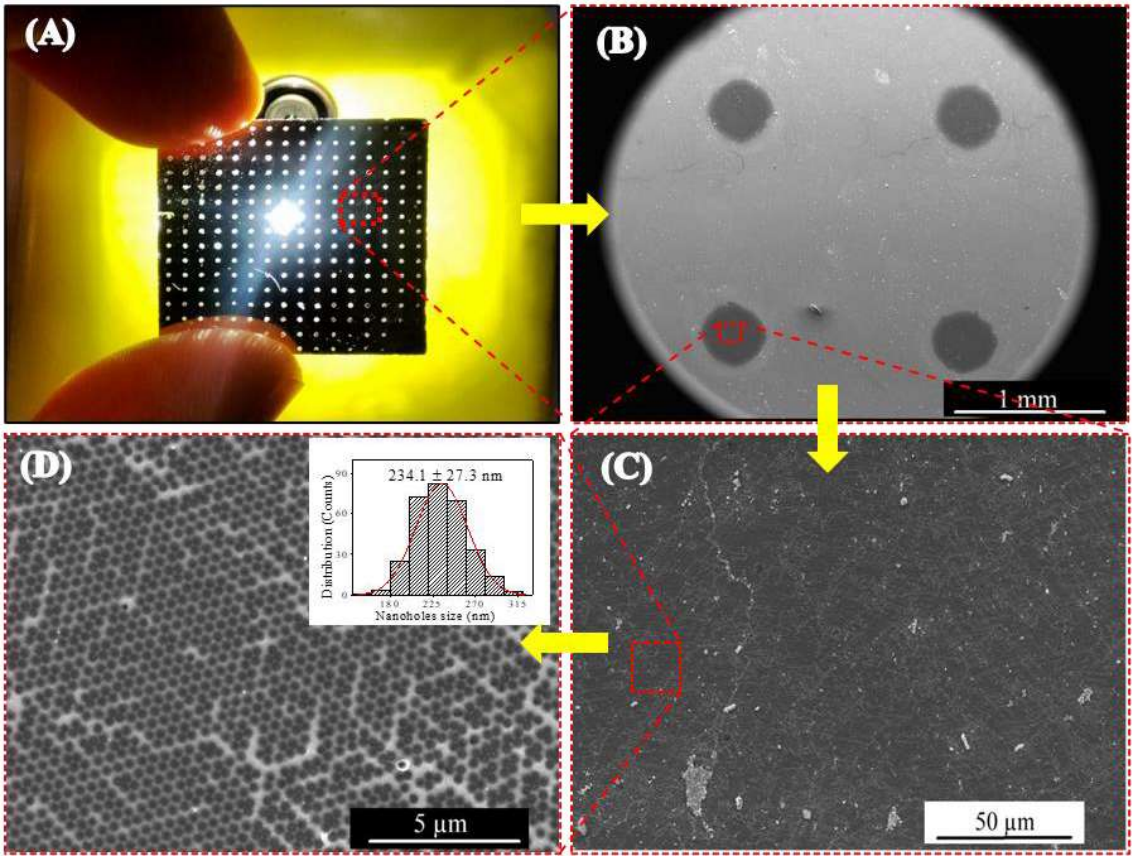

Fig. 2. (A) digital image of the demarcated substrate, (B) SEM image of the four Sen-Ps indicated in (A), and (C-D) show SEM images at different magnifications obtained within the Sen-P area. Inset in (D) shows a nanoholes size distribution obtained from the (D) image.

The evaluation of the Sen-P optical transmission revealed a plasmonic band at a 531 nm maximum wavelength when a dilute glucose solution (RI=1,3397) was on it. This behavior was the same observed for other substrate Sen-Ps. The maximum transmission wavelength was close to the one observed in our previous work [11]. As observed in Fig. 3(A)-3(B), the transmission spectra were red-shifted as the RI increased. Then, the sensitivity (S) was determined using a linear fitting of the maximum transmission wavelength as a function of RI variation. The fitting curve inclination is defined as the Sen-P sensitivity (Fig. 3(C)), which was (271.92 ± 14.92) nm/RIU. Considering that the spectrophotometer precision was 0.1 nm, the calculated resolution was 3.7 x 10^{-4} RIU. Moreover, the R^2 for the linear fitting was acceptable (0.9764), indicating that the transmission maximum wavelength shift is proportional to RI changes.

The device response to the biomolecule immobilization was also investigated using the traditional model system of MUA/NHS-BSA [12]. The MUA-NHS layers are extensively used to provide a compact layer on the gold surface [13]. The BSA aminated groups quickly adsorb

on the MUA/NHS-modified gold surface and form a 4-7 nm thick monolayer [14] (see Figure S1 in the supplementary material). Thus, this molecular system can determine the substrate's ability to evaluate the sensor surface layer-by-layer modification. This is important to define if the substrate can work as a biosensor. The Sen-P transmission spectra were acquired for each modification step. The region of the spectra maximum absorbance can be observed in Figure 3(D). The Fig. 3(D) inset shows the plasmonic band maximum wavelength for each modification. The redshift caused by the immobilization of the NHS layer over MUA was only (0.6±0.22) nm. However, a significant shift of (2.48±0.57) nm was observed when BSA molecules were immobilized on MUA-NHS layer. According to these results, and the literature support (supplementary information) the device has potential to detect surface biological interactions and also work as a plasmonic biosensor.

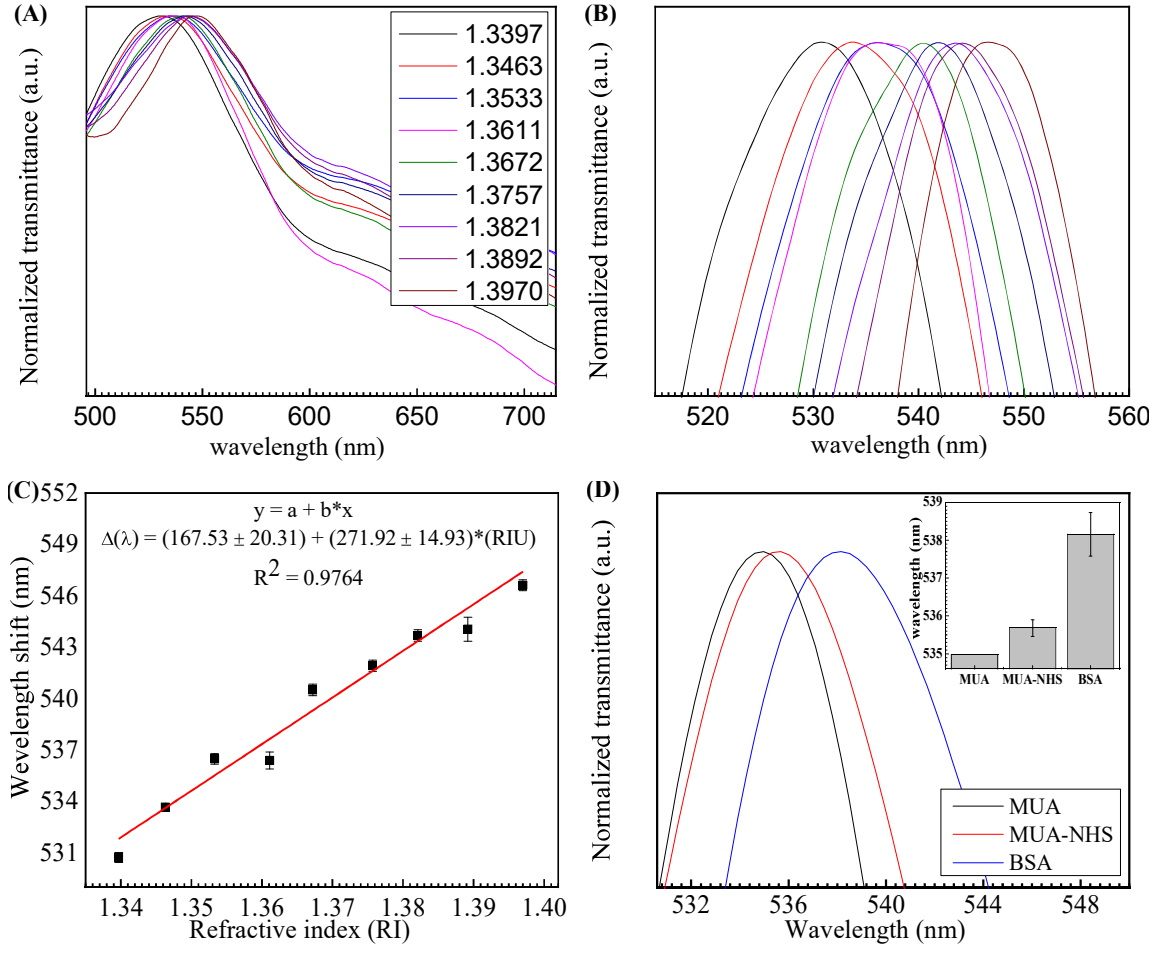

Fig. 3. (A) Transmission spectra for a Sen-P at different IRs (1.3397-1.3970). (B) Expansion of the maximum absorbance region observed in (A). (C) Maximum transmission wavelength as a function of RI variation (sensibility curve). (D) Transmission spectra for each step of the gold surface modification on the Sen-P. Inset: column chart to plasmonic band redshift.

4. Conclusion

In this work, we presented a new nanoholes-based plasmonic substrate obtained by a facile technique. The substrate was successfully prepared with several Sen-Ps with a circular area filled with hexagonal-shaped nanoholes on gold thin film. The Sen-Ps were obtained using a polymeric coating followed by remotion and then obtaining the plasmonic platform with a multiplexing potential. The Sen-P arrays can be fully customized. It was shown that the device was sensitive to RI changes and can respond to the biomolecules immobilization. The results demonstrated that combining the techniques (nanohole development by NSL and demarcation with an easy-to-remove polymeric system) enables the acquisition of plasmonic substrate with the potential for multiple detections at a label-free single device.

Acknowledgement

The authors thank the Complex of Research Support Centers (COMCAP) for equipment support, CNPq (process no. 305290/2020-7) and CAPES for fellowships.

References

[1] J. Homola, Surface Plasmon Resonance Sensors for Detection of Chemical and Biological Species, Chem. Rev. 108 (2008) 462–493. https://doi.org/10.1021/cr068107d.

[2] C. Escobedo, On-chip nanohole array-based sensing: a review, Lab Chip. 13 (2013) 2445. https://doi.org/10.1039/c3lc50107h.

[3] P.H.M. Buzzetti, M.M. Taniguchi, N.S. Mendes, R.C. Vicentino, J.H. Oliveira, B.P. Cabral Júnior, M. Souza, J.P. Monteiro, E.M. Girotto, Complete experimental and theoretical characterization of nonlinear concentration gradient generator microfluidic device for analytical purposes, Microchim. Acta. 11 (2022) 1–9. https://doi.org/10.1007/s00604-021-05110-7.

[4] A. Shalabney, I. Abdulhalim, Sensitivity-enhancement methods for surface plasmon sensors, 606 (2011) 571–606. https://doi.org/10.1002/lpor.201000009.

[5] P. Colson, C. Henrist, R. Cloots, Nanosphere Lithography: A Powerful Method for the Controlled Manufacturing of Nanomaterials, 2013 (2013) https://doi.org/10.1155/2013/948510.

[6] J.M. Chem, Elevated Ag nanohole arrays for high performance plasmonic sensors based on extraordinary optical transmission, (2012) 8903–8910. https://doi.org/10.1039/c2jm30525a.

[7] L. Niu, K. Cheng, Y. Wu, T. Wang, Q. Shi, D. Liu, Z. Du, Sensitivity improved plasmonic gold nanoholes array biosensor by coupling quantum-dots for the detection of specific biomolecular interactions, Biosens. Bioelectron. 50 (2013) 137–142. https://doi.org/10.1016/j.bios.2013.06.023.

[8] S. Su, L. Lin, Z. Li, J. Feng, Z. Zhang, The fabrication of large-scale sub-10-nm core-shell silicon nanowire arrays, Nanoscale Res. Lett. 8 (2013) 405. https://doi.org/10.1186/1556-276X-8-405.

[9] Y. Cai, Y. Cao, P. Nordlander, P.S. Cremer, Fabrication of Split-Rings via Stretchable Colloidal Lithography, ACS Photonics. 1 (2014) 127–134. https://doi.org/10.1021/ph400127g.

[10] Z. Zhao, J. Wu, X. Mu, H. Chen, H.J. Qi, D. Fang, Origami by frontal photopolymerization, Sci. Adv. 3 (2017) 1–8. https://doi.org/10.1126/sciadv.1602326.

[11] B.P. Cabral Júnior, J.H. Oliveira, P.H.M. Buzzetti, M.G.V. Fressatti, J.P. Monteiro, L.H.C. Amorin, A. Urbano, E. Radovanovic, E.M. Girotto, Cost-effective plasmonic device for label-free streptavidin detection, Mater. Lett. 227 (2018) 243–246. https://doi.org/10.1016/j.matlet.2018.05.064.

[12] C.T.P. Silva, J.P. Monteiro, E. Radovanovic, E.M. Girotto, Unprecedented high plasmonic sensitivity of substrates based on gold nanoparticles, Sensors Actuators B Chem. 191 (2014) 152–157. https://doi.org/10.1016/j.snb.2013.09.109.

[13] J.P. Monteiro, J. Ferreira, R.G. Sabat, P. Rochon, M.J.L. Santos, E.M. Girotto, SPR based biosensor using surface relief grating in transmission mode, Sensors Actuators B Chem. 174 (2012) 270–273. https://doi.org/10.1016/j.snb.2012.08.026.

[14] H. Guner, E. Ozgur, G. Kokturk, M. Celik, E. Esen, A.E. Topal, S. Ayas, Y. Uludag, C. Elbuken, A. Dana, A smartphone-based surface plasmon resonance imaging (SPRi) platform for on-site biodetection, Sensors Actuators B Chem. 239 (2017) 571–577. https://doi.org/10.1016/j.snb.2016.08.061.